

## Distinguishing Manuel Panselinos from Michael Astrapas and Eutybios: A CIELAB Color Analysis of 13th Century Macedonian School Frescoes

Antigoni Vlisidi<sup>1</sup>, Apostolos Vlyssides<sup>2</sup>

### Abstract

The chromatic analysis of frescoes using the CIELAB method represents a novel, non-destructive approach for the preliminary study of an artist, based on the colorimetric analysis of their work as a whole. By employing sophisticated mathematical relationships, this method reveals an artist's color preferences and tendencies, which appear to be unique to each individual. Quantifying these preferences through CIELAB analysis allows for the establishment of a personal "color identity" expressed through stochastic mathematical relations. Consequently, the effective disclosure of these chromatic profiles requires the analysis of a sufficient number of representative images. Applying these principles to a case study of two prominent 13th-century masters of the Macedonian School, Manuel Panselinos and the Michael Astrapas and Eutybios, this research demonstrated a strong, individual linear correlation between the chromatic variable  $\Delta C^*$  and the variable  $\Delta b^*$  in their respective paintings. This linear relationship serves as a unique chromatic property for each painter, constituting a distinct "color signature." The establishment of a comprehensive database utilizing the CIELAB method to register these chromatic signatures could prove invaluable for the attribution of unsigned works. This potential was validated in the present study, which confirmed the hypothesis that Panselinos was the artist responsible for the unsigned frescoes in the Chapel of Saint Eftymios in Thessaloniki. Ultimately, the creation of a global CIELAB-based chromatic database for artists and their frescoes would significantly facilitate the further study and authentication of Byzantine monumental painting.

**Keywords:** *Art, CIELab Colorimetric Method, Macedonian Hagiography School, Panselinos M., Astrapas M.*

### Introduction

Byzantine Iconography is the pictorial depiction of saints and religious scenes inspired by the Synaxaria and the lives of the Saints. This art form emerged during the early years of the Byzantine Empire, a period when the Emperor held absolute authority, and matured through significant theological transitions, most notably the conflict between iconolatry and iconoclasm. In the art of iconography, there are strict rules and aesthetic codes that every iconographer must follow to methodically achieve the intended spiritual outcome. Ultimately, an icon is not merely a religious painting, but a composition imbued with profound symbolism [1].

In the depiction of religious subjects, specific iconographic rules have been established. It is mandatory for iconographers to faithfully reproduce the physical characteristics of sacred figures, as these have been handed down through early hagiographic texts or various visual models known as "archetypes." Consequently, this practice has resulted in the cross-century repetition of a strictly defined formula for each holy person [2]. Furthermore, it is essential that the figures exude a deep sense of spirituality. Saints are depicted as solemn yet merciful, never smiling and devoid of any secular expression. Byzantine iconography primarily draws its themes from the Old Testament, the Gospels, and the lives of the Saints. A prime example of these rigorous aesthetic standards is the prohibition of shadows; every element is rendered bright and distinct, as if illuminated by the "Uncreated Light" of God. This divine light effectively abolishes the constraints of cosmic space and time. Consequently, elements separated by vast chronological distances are often unified within a single composition. In this

<sup>1</sup> Department of Materials Science and Engineering, School of Chemical Engineering, National Technical University of Athens, Greece

<sup>2</sup> Organic Chemical Technology Lab in National Technical University of Athens, Greece (Corresponding Author)

tradition, the scale of objects does not adhere to linear perspective based on proximity to the viewer. Instead, size is determined by the hierarchical importance of the subject, transcending temporal and spatial limitations. This is further emphasized by the fact that all environmental elements, including mountains, are oriented toward the center of the icon, utilizing what is known as "reverse perspective." Ultimately, in the art of the icon, conventional space, time, and perspective are entirely abolished in favour of a spiritual representation [2].

Within these rigorous frameworks, an artist has limited scope to develop a highly individualized painting style that would be easily recognizable at first glance. However, a significant degree of creative freedom lies in the application of color. This latitude allows each artist, whether consciously or subconsciously, to establish a distinct pattern of colors and shades across their entire body of work. Consequently, by analysing these chromatic patterns through appropriate statistical techniques, the unique artistic "signature" of the iconographer can be effectively revealed [3, 4, 41].

The most prevalent method for expressing color measurements is the L\*a\*b\* color space [5], which encompasses two primary models: the CIE 1976 (CIELAB) and the Hunter model [6, 7]. While the latter employs "square root" coordinates, the CIELAB model utilizes "cubic root" coordinates and is the most widely adopted [8]. A key advantage of the CIELAB system is that its gradation closely aligns with human color perception. The CIELAB method is effectively utilized across various industrial sectors, such as food quality assessment [9, 10, 11] and biological process control, where product color is inherently linked to quality [12]. Recently, the development of lightweight, portable instruments—such as spectrophotometers—has enabled in-situ, non-destructive measurements, making colorimetric analysis highly attractive for the study of cultural heritage monuments. This approach provides rapid results, facilitates statistical processing, and allows for comparative studies with historical data from the same or similar monuments. The CIELAB system is structured around three axes: L\* (lightness/darkness), a\* (red/green), and b\* (blue/yellow) [13]. The direct measurement of these fundamental variables, alongside calculated derivatives such as  $\Delta L^*$ ,  $\Delta a^*$ ,  $\Delta b^*$ ,  $\Delta h^\circ$ ,  $\Delta C^*$ , and  $\Delta E^*$  (Table 1), provides a robust tool for the mathematical expression of an image's chromatic characteristics [14, 15, 16]. Ultimately, the cross-correlation of these chromatic variables, when collected from a sufficient corpus of an iconographer's work, can reveal their unique and specific artistic signature.

**Table 1. The CIELAB Variables Used in This Study**

Variables	Equation/description	References
L*	Lightness ranging from 0 (black) to 100 (white).	[5]
	Difference $\Delta L^* = L^*_{\text{sample}} - L^*_{\text{standard}}$	
a*	Green/red component ranging from negative (green) to positive (red) values.	[5]
	Difference $\Delta a^* = a^*_{\text{sample}} - a^*_{\text{standard}}$	
b*	Blue/yellow component ranging from negative (blue) to positive (yellow) values	[5]
	Difference $\Delta b^* = b^*_{\text{sample}} - b^*_{\text{standard}}$	
Hue (h°)	$h^\circ = \tan^{-1}(b^*/a^*)$	[17]
	Difference $\Delta h^\circ = \tan^{-1}(\Delta b^*/\Delta a^*)$	
Chroma (C*)	$C^* = (a^{*2} + b^{*2})^{0,5}$	[18]
	Difference $\Delta C^* = (\Delta a^{*2} + \Delta b^{*2})^{0,5}$	
Chromatic quotient	$\Delta a^*/\Delta b^*$	[18]
Total color E*	$E^* = (L^{*2} + a^{*2} + b^{*2})^{0,5}$	[19]
	Difference $\Delta E^* = (\Delta L^{*2} + \Delta a^{*2} + \Delta b^{*2})^{0,5}$	

$\Delta(\text{variable})$	Differences between the measured correspondence variable from spectrophotometer and correspondence substrate of every image. This difference eliminates the possible effects of the image substrate and homogenizes the results.
---------------------------	--

Furthermore, non-destructive testing (NDT), with a particular emphasis on spectral imaging within the visible spectrum, represents the cutting edge of diagnostic methodologies. It serves as a vital tool for art historians, scholars, conservators, and researchers alike [20].

The CIELAB method, as a non-invasive technique, is particularly advantageous due to its rapid in-situ application and the absence of costly consumables. It allows for the comprehensive inspection of an object's entire surface and provides mapping capabilities, enabling the examination of extensive areas within an image [21, 22]. The CIELAB color space has already been successfully employed to quantify the temporal deterioration of monuments and statues [23, 24, 25]. Additionally, spectral and multispectral image analysis have been utilized as simple, cost-effective methods for the formulation and design of specialized conservation paints [26, 27, 28].

## Material and Methods

### Chromatic Analysis of Fresco Images via the CIELAB Color Model

Color measurements were performed using a Dr. Lange spectrophotometer (Hach Lange LMG 183), a portable colorimetric device. The instrument utilizes a standard  $d/8^\circ$  circular viewing geometry and a D65/10 $^\circ$  illuminant. Before each measurement session, the device was calibrated using two reference standards (LZM 268): a black standard ( $X=4.07, Y=4.35, Z=4.59$ ) and a white standard ( $X=83.78, Y=88.60, Z=90.39$ ). The spectrophotometer's sensors, equipped with specialized filters, simulate the tristimulus response of the human eye, with color detection achieved through an integrated artificial light source.

To measure the primary color variables ( $L^*$ ,  $a^*$ , and  $b^*$ ), each image, regardless of its original dimensions, had to be scaled to a uniform area of  $2.5 \times 2.5$  cm, corresponding to the field of view of the LMG 183 spectrophotometer. This resizing was performed using the advanced capabilities of CorelDRAW graphic design software. By employing this scaling method, the qualitative and quantitative ratios of the colors remain constant, ensuring that the colorimetric values are preserved while representing the chromatic profile of the entire image.

Consequently, the fresco images were analyzed using the CIELAB color model, a visually uniform 3-D color space defined by three coordinates:  $L^*$  indicates lightness, ranging from 0 (black) to 100 (white);  $a^*$  represents the green/red component (negative for green, positive for red); and  $b^*$  represents the blue/yellow component (negative for blue, positive for yellow) [29, 30]. Furthermore, the hue angle  $h^\circ$  [17], Chroma  $C^*$  [18], and the total color difference  $\Delta E^*$  [19]—all derived from the CIELAB model—were calculated according to the mathematical relationships presented in Table 2.

The color of each fresco image was determined by averaging three consecutive measurements (shots) from the spectrophotometer's illuminant to ensure accuracy. The fundamental color variables  $L^*$ ,  $a^*$ , and  $b^*$  were instantly displayed on the device's screen, while the remaining CIELAB parameters ( $\Delta h^\circ$ ,  $\Delta C^*$ , and  $\Delta E^*$ ) were derived using the mathematical equations presented in Table 1.

The primary objective of this study was to perform a chromatic analysis via the CIELAB method on a representative corpus of frescoes by two distinguished 13th-century Byzantine masters: Manuel Panselinos and the duo Michael & Eutybios Astrapas. Through the mathematical processing of these variables, the research aimed to identify the distinct color expression of each artist, as well as any underlying commonalities in their color design. This comparative analysis is particularly significant, as both workshops belonged to the same artistic tradition—the Macedonian School—and were active during the same period (late 13th to early 14th century) [24].

### 1st Case Study: Paintings of Manuel Panselinos

To investigate whether an artist follows a distinct, personal color pattern—consciously or subconsciously—across their entire body of work, this research focuses on the CIELAB color parameters of thirty representative works by Manuel Panselinos. A preeminent Byzantine master of the Palaeologan Renaissance, Panselinos is renowned for introducing emotional depth (pathos) into the

frescoes and icons of the late 13th and early 14th centuries. Based in Thessaloniki, the second-largest city of the era, he is widely regarded as the most influential figure of the Macedonian School of painting [30]. Born in Thessaloniki in the late 13th century, Panselinos dedicated his career to monumental fresco painting and iconography. His most significant works are preserved in several monasteries of Mount Athos, including Vatopedi, Megisti Lavra, and most notably, the Protaton Church in Karyes, which houses his masterwork [31, 32, 33]. Art historians have long identified a singular stylistic identity in his oeuvre, characterized by the use of soft color palettes, the symmetrical rendering of figures, and a unique approach to composition and proportions, particularly in the depiction of faces. The thirty icons and frescoes selected for this study [34] are illustrated in Figure 1.

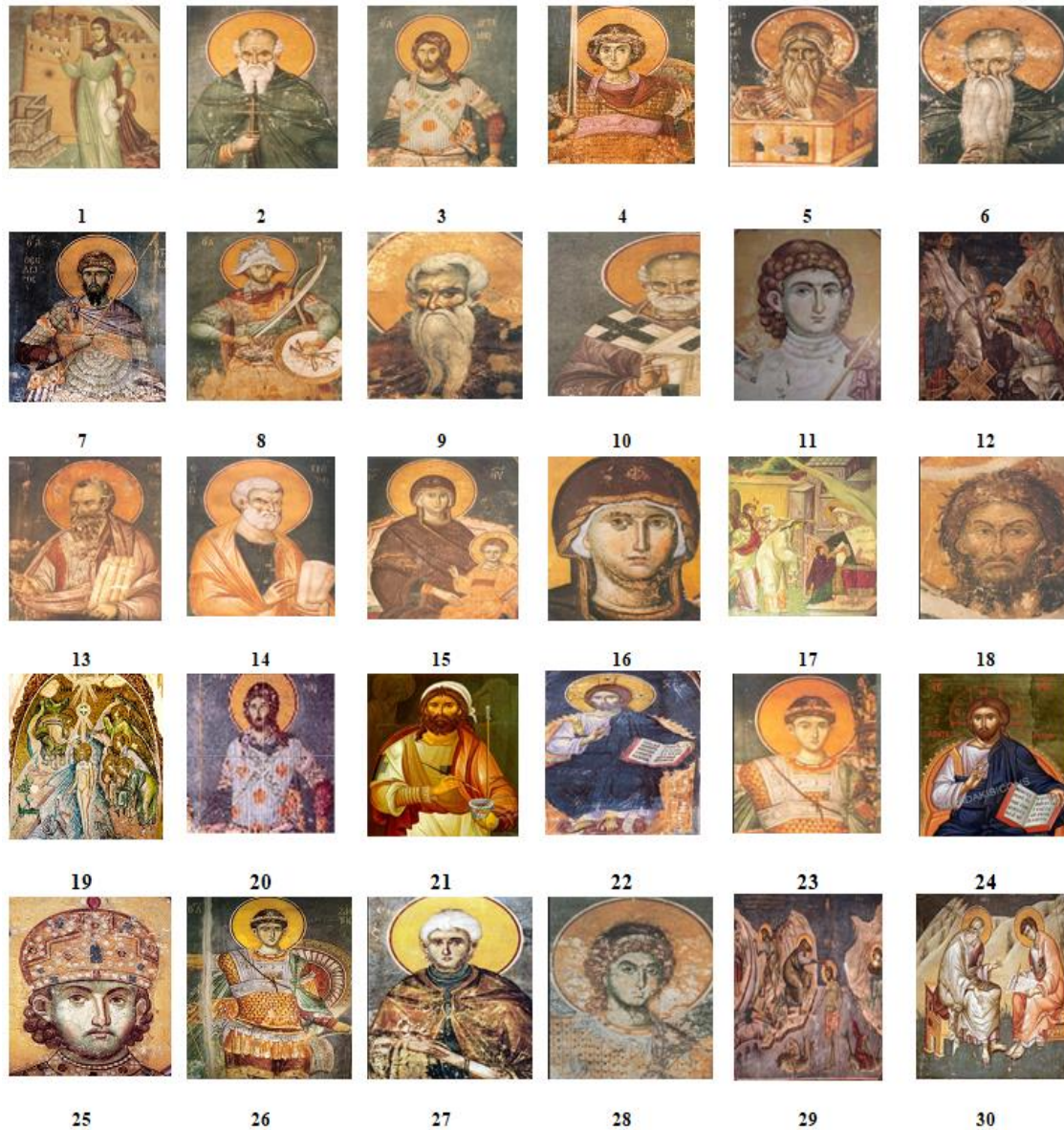


**Figure 1:** Hagiographies by Manuel Panselinos that included in this research

## **2<sup>d</sup> Case Study: Paintings of Michael and Eftychios Astrapas**

Michael Astrapas and Eutybios are among the few painters of the Byzantine era whose signatures have been preserved to the present day [35]. Their artistic output has been linked to numerous mural cycles across Serbia, North Macedonia, and Greece. The distinct qualities of their style represent one of the most significant artistic currents of the late 13th and early 14th centuries, often referred to as the "First Palaeologan Renaissance" or the "Voluminous Style" (Mannerism). Specifically, the wall paintings examined in this research belong to the following monuments: the Church of Panagia Perivleptos in Ohrid, the Žiča Monastery in Serbia, the Monastery of Panagia Olympiotissa in Ellassona (Greece), the

Monastery of St. Prochoros Pčinjski in Serbia, the Chapel of Sts. Joachim and Anne at the Studenica Monastery, the Church of St. George at Staro Nagoričino, the Banjska Monastery, and the Monastery of St. Nikita in Čučer. These eight monuments are either directly attributed to the workshop of Michael Astrapas and Eutybios or are closely associated with their artistic guild. The thirty icons and frescoes selected for this study [36] are illustrated in Figure 2.

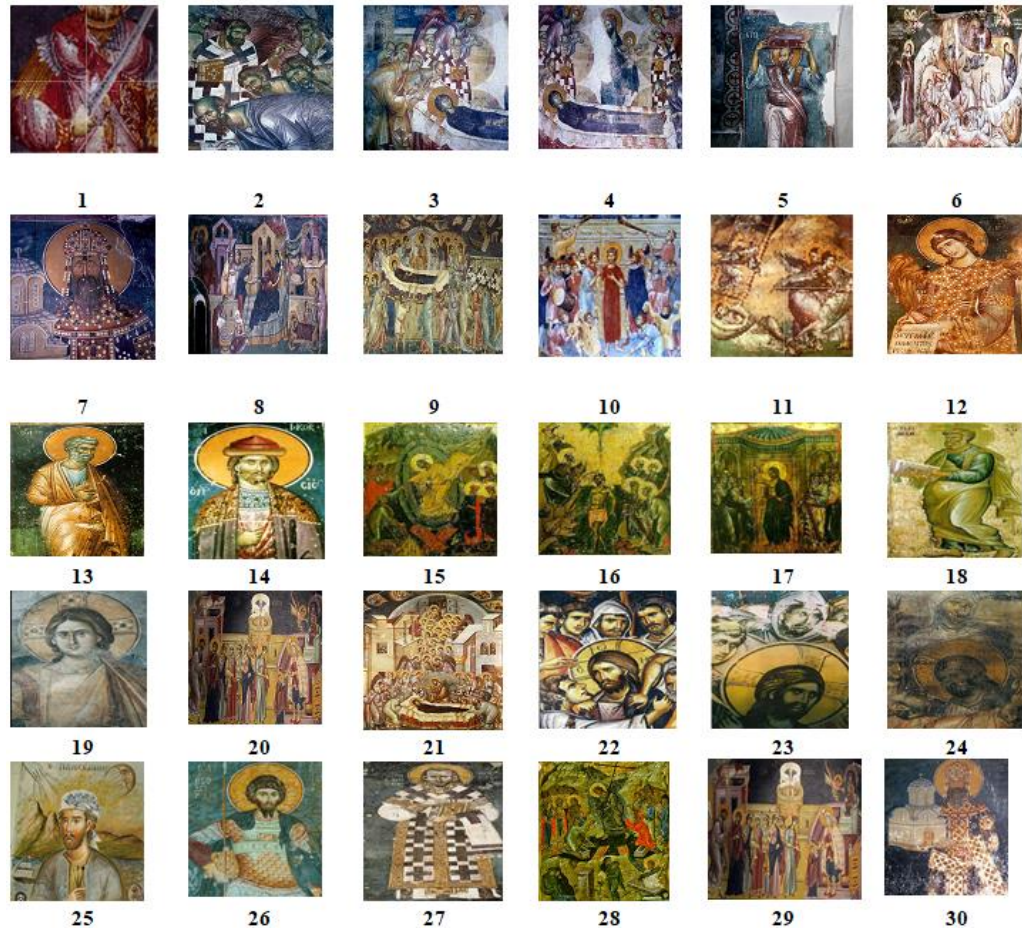


**Figure 2:** Hagiographies by Michael and Eftybios Astrapas are included in this research

### Regression Analysis

Statistical regression analysis was employed to evaluate the relationships between the CIELAB color variables and their respective standard deviations. Linear regression models were tested to identify the strongest correlations among variables, as expressed by Pearson’s correlation coefficient (R<sup>2</sup>). The objective was to achieve the highest possible R<sup>2</sup> value [37, 38] while maintaining the lowest feasible standard deviation. The existence of a strong linear relationship among CIELAB variables—characterized by a high R<sup>2</sup> coefficient and a correspondingly low standard deviation—serves as compelling evidence that an iconographer possesses a distinct, personal method of color application. The primary aim of the investigation presented in this paper is to provide empirical proof of this unique chromatic signature for each hagiographer.

### Results and Discussion

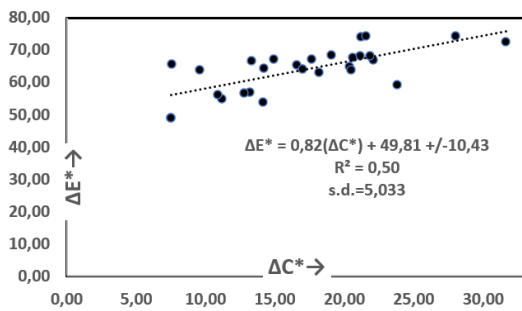
#### Analysis of CIELAB variables for the hagiographies of M.Panselinos

The measured (L\*,a\*,b\*) and calculated ( $\Delta h^{\circ}$ ,  $\Delta C^*$ ,  $\Delta E^*$ ) CIELAB variables for the iconographic images shown in Figure 1 are summarized in Table 2. Figure 3 illustrates the most statistically significant linear relationships between these variables. Additionally, Table 3 presents the corresponding correlation coefficients and their respective standard deviations for each of these relationships.

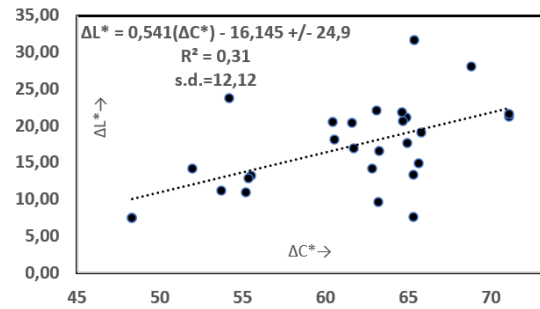
**Table 2: Results of Measurement and Calculations of Variables for the Pancelinos' Hagiographies**

No of image	$\Delta L^*$	$\Delta a^*$	$\Delta b^*$	$\Delta h^*$	$\Delta C^*$	$\Delta E^*$					
1	5	71,0	9,4	19	-2,07	0	21,2	4	74,1		
2	7	71,0	9,45	5	19,3	-1,94	3	21,5	6	74,2	
3	7	61,5	7,41	4	18,9	-0,66	4	20,3	4	64,8	
4		63,1	8,97	5	20,1	-1,25	6	22,0	4	66,8	
5	1	60,5	7,85	5	16,3	-1,78	4	18,1	7	63,1	
6	9	65,7	7,6	9	17,4	-1,12	7	19,0	0	68,5	
7	3	51,9	6,06	6	12,7	-1,69	3	14,1	2	53,8	
8	2	60,4	8,29		18,7	-1,22	6	20,4	9	63,7	
9	3	64,9	6,5	7	16,3	-0,72	1	17,6	8	67,2	
10	6	64,8	7,76	5	19,6	-0,70	3	21,1	1	68,2	
11	7	65,6	7,09	6	15,5	-1,77	9	17,7	5	68,2	
12	9	53,6	5,23		9,84	-3,11	4	11,1	3	54,8	
13	4	64,6	9,91	5	18,0	-3,91	9	20,5	4	67,8	
14	9	68,7	13,9	5	8	24,2	-5,84	0	28,0	7	74,2
15		64,6	9,57	4	19,6	-1,91	5	21,8	9	68,1	
16	2	61,7	5,85	3	15,9	-0,44	7	16,9	1	64,0	
17	2	65,6	4,5		14,2	0,01	0	14,9	9	67,2	
18		55,5	6,19	1	11,6	-3,18	6	13,1	4	57,0	
19	9	63,1	2,34		9,29	1,09		9,58	1	63,9	
20	8	54,1	10,0	4	7	21,5	-1,53	9	23,7	7	59,1
21	7	55,1	3,39	2	10,3	-0,10	6	10,8	3	56,2	
22	4	65,3	16,3	4	8	27,0	-	3	31,6	9	72,5
23	2	48,3	3,13		6,81	-1,45		7,49	0	48,9	
24		65,3	3,65		6,63	-3,99		7,57	4	65,7	
25	2	48,3	3,13		6,81	-1,45		7,49	0	48,9	
26	1	62,8	6,13	7	12,7	-1,78	7	14,1	9	64,3	
27		65,3	3,66	8	12,7	0,37	9	13,2	4	66,6	

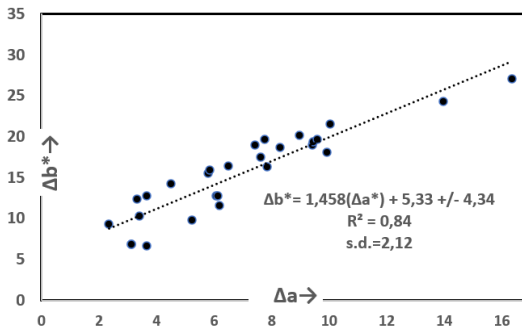
28	5	55,3	3,32	4	12,3	0,65	8	12,7	1	56,8
29	3	54,1	5,22		3,97	0,95		6,56	3	54,5
30	2	68,2	4,97	7	13,1	-0,54	8	14,0	6	69,6
Mean value	7	65,6	7,09	6	15,5	-1,77	9	17,7	5	68,2
Standard Deviation (s.d.)		7,68	3,35		5,71	2,40		6,29		8,45



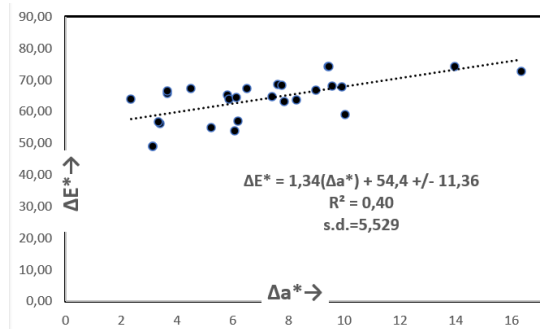
3A: Linear relation between  $\Delta E^*$  and  $\Delta C^*$



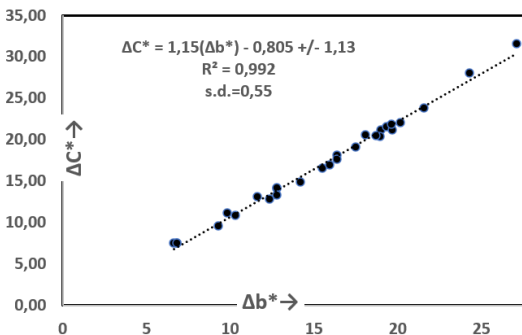
3B: Linear relation between  $\Delta L^*$  and  $\Delta C^*$



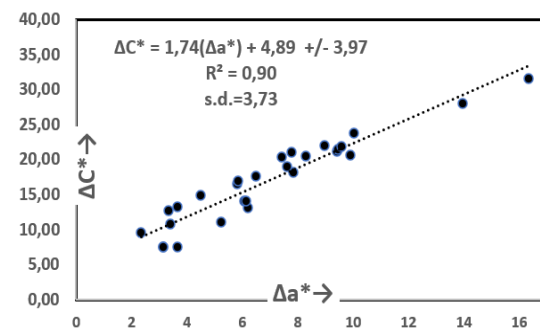
3C: Linear relation between  $\Delta b^*$  and  $\Delta a^*$



3D: Linear relation between  $\Delta E^*$  and  $\Delta a^*$



3E: Linear relation between  $\Delta C^*$  and  $\Delta b^*$



3F: Linear relation between  $\Delta C^*$  and  $\Delta a^*$

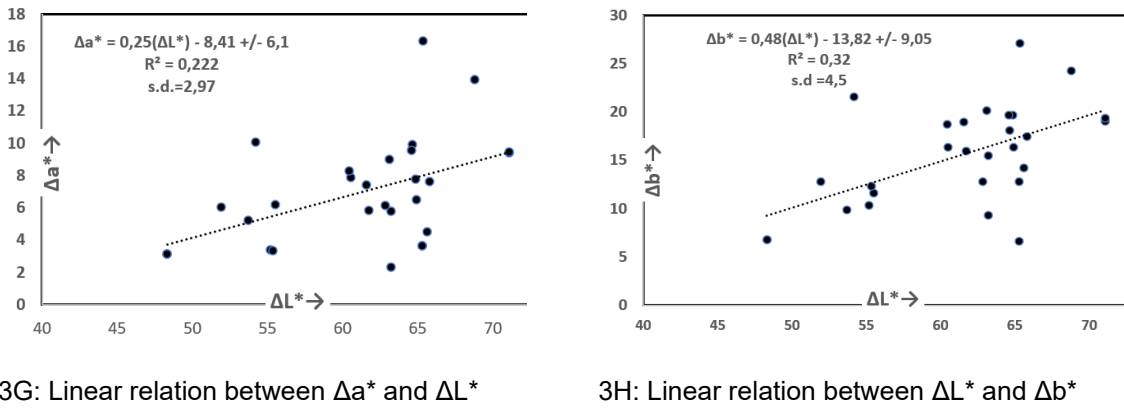


**Figure 3:** The most interesting linear relations between CIELAB variables of the examined thirty frescoes painted by M. Panselinos

**Table 3: Correlation coefficients R2 and standard deviation (s.d.) of the linear relations between CIELAB variables calculated from the results of the table 2**

	$\Delta L^*$		$\Delta a^*$		$\Delta b^*$		$\Delta h^*$		$\Delta C^*$		$\Delta E^*$	
	R <sup>2</sup>	s.d.	R <sup>2</sup>	s.d.	R <sup>2</sup>	s.d.	R <sup>2</sup>	s.d.	R <sup>2</sup>	s.d.	R <sup>2</sup>	s.d.
$\Delta L^*$	-	-	0,22	2,97	0,32	4,5			0,31	12,1		
$\Delta a^*$	0,222	2,97	-	-	0,84	2,12			0,9	3,73	0,4	5,53
$\Delta b^*$	0,32	4,5	0,84	2,12	-	-			0,992	0,55		
$\Delta h^*$							-	-				
$\Delta C^*$	0,31	12,1	0,9	3,73	0,992/	0,55			-	-	0,5	5,03
$\Delta E^*$			0,4	5,53					0,5	5,03	-	-

Based on the results presented in Table 3, the best fit among these relationships is observed in Figure 3E ( $\Delta b^* \rightarrow \Delta C^*$ ), yielding a coefficient of determination  $R^2 > 0.99$ , a standard deviation  $s.d. = 0.55$ , and a slope of 1.15. These values indicate that the overall chromatic profile of Panselinos' icons is predominantly characterized by yellow hues, with a significantly lower contribution from other colors. Furthermore, the relationships depicted in Diagrams 3B, 3G, and 3H demonstrate that the lightness of the images ( $\Delta L^*$ ) does not significantly influence the overall color composition. Additionally, the correlation shown in Figure 3C ( $\Delta b^* \rightarrow \Delta a^*$ , with  $R^2 > 0.84$  and  $s.d. = 2.12$ ) suggests that the iconographer maintains a relatively constant color ratio throughout his oeuvre.

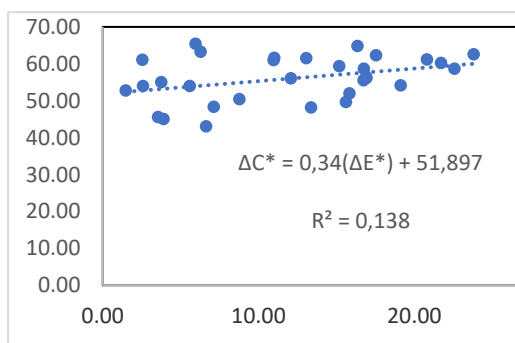
**Analysis of CIELAB variables for the fresco images of Michael Astrapas and Eutychios**

The measured ( $L^*, a^*, b^*$ ) and calculated ( $\Delta h^*, \Delta C^*, \Delta E^*$ ) CIELAB variables for the iconographic images illustrated in Figure 1 are summarized in Table 4. The most statistically significant linear relationships between these variables are depicted in Figure 5. Furthermore, Table 5 presents the corresponding correlation coefficients and their respective standard deviations for these relationships.

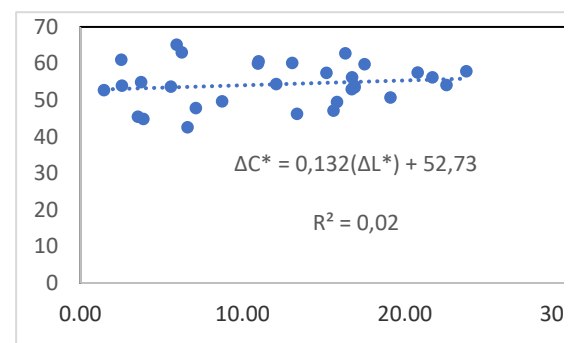
**Table 4: Results of measurements and calculations of variables for Michael and Eutychios Astrapas hagiographies**

No of image	$\Delta L^*$	$\Delta a^*$	$\Delta b^*$	$\Delta h^*$	$\Delta C^*$	$\Delta E^*$
1	47,75	7,14	-0,15	-0,02	7,14	48,28
2	45,36	2,34	2,69	2,23	3,57	45,50
3	60,96	2,44	-0,73	-0,31	2,55	61,01
4	53,65	-1,52	-5,39	0,43	5,60	53,94
5	52,69	-1,14	0,96	-1,12	1,49	52,71

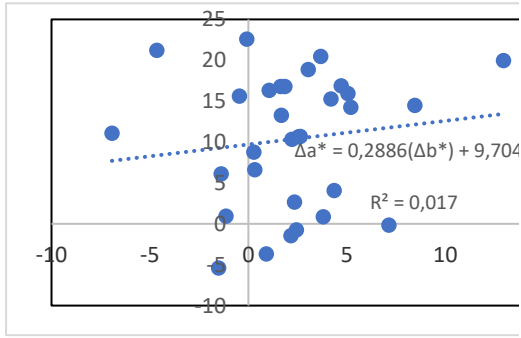
6	65,10	4,36	4,08	1,36	5,97	65,37
7	44,82	3,81	0,87	0,23	3,91	44,99
8	53,90	2,17	-1,42	-0,77	2,59	53,96
9	49,62	0,27	8,77	1,81	8,77	50,39
10	54,86	0,91	-3,66	-1,21	3,77	54,99
11	56,13	8,45	14,49	-6,90	16,77	58,58
12	57,83	12,96	19,99	35,25	23,82	62,54
13	52,89	5,05	15,97	0,02	16,75	55,48
14	62,72	1,05	16,33	-0,16	16,36	64,82
15	54,09	-0,08	22,60	0,25	22,60	58,62
16	50,62	3,04	18,90	-0,07	19,14	54,12
17	46,19	1,68	13,28	-19,68	13,39	48,09
18	56,16	-4,65	21,22	-6,66	21,72	60,22
19	62,95	-1,39	6,13	-3,21	6,29	63,26
20	59,74	4,72	16,90	0,47	17,55	62,26
21	57,36	5,21	14,27	-0,43	15,19	59,34
22	53,85	1,65	16,83	0,98	16,91	56,44
23	57,48	3,68	20,50	-0,86	20,83	61,14
24	42,47	0,32	6,63	-3,25	6,64	42,99
25	53,45	1,85	16,83	-0,34	16,93	56,07
26	60,12	-6,93	11,10	32,32	13,09	61,53
27	59,93	2,55	10,68	1,73	10,98	60,93
28	47,10	-0,45	15,62	-0,15	15,63	49,62
29	60,55	2,64	10,69	1,28	11,01	61,54
30	49,43	4,19	15,29	0,56	15,85	51,91
Mean value	54,33	2,21	10,34	1,13	12,09	56,02
Standard Deviation (s.d.)	5,92	3,75	8,20	9,77	6,77	6,20



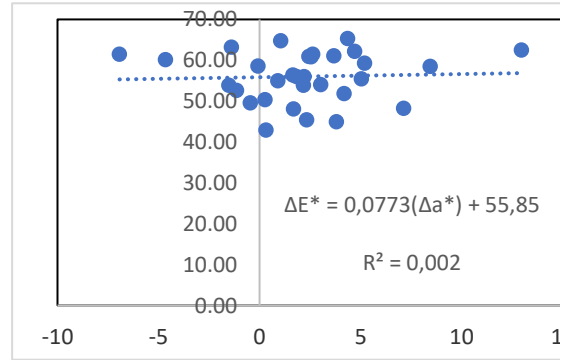
4A: Linear relation between  $\Delta E^*$  and  $\Delta C^*$



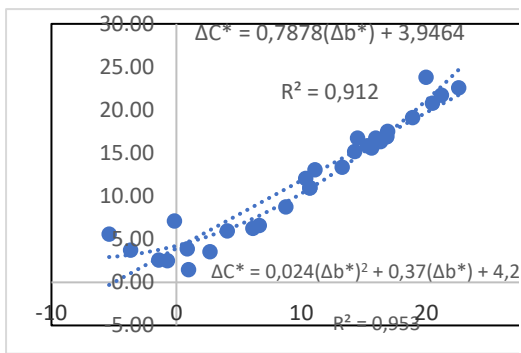
4B: Linear relation between  $\Delta L^*$  and  $\Delta C^*$



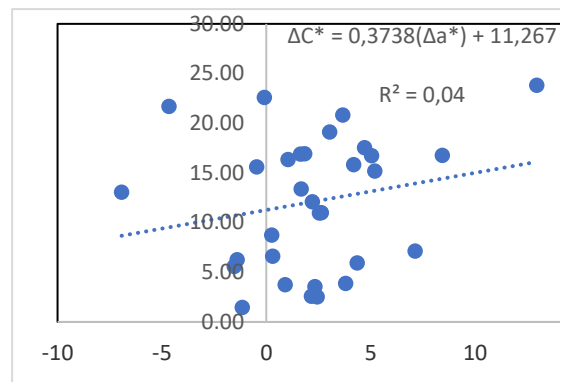
4C: Linear relation between  $\Delta b^*$  and  $\Delta a^*$



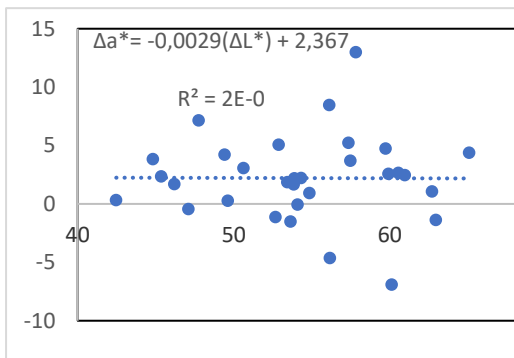
4D: Linear relation between  $\Delta E^*$  and  $\Delta a^*$



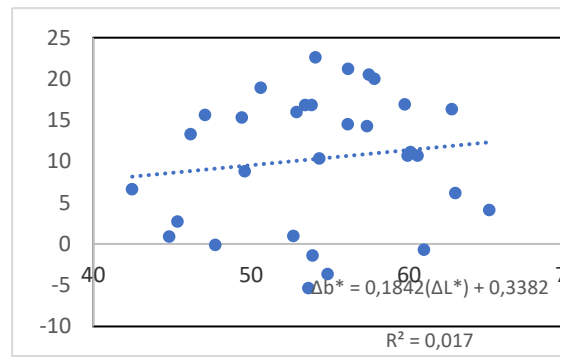
4E: Linear relation between  $\Delta C^*$  and  $\Delta b^*$



4F: Linear relation between  $\Delta C^*$  and  $\Delta a^*$



4G: Linear relation between  $\Delta a^*$  and  $\Delta L^*$



4H: Linear relation between  $\Delta L^*$  and  $\Delta b^*$

**Figure 4:** The most interesting linear relations between CIELAB variables of the examined thirty frescoes painted by Michael and Eutychios Astrapas

**Table 5: Correlation coefficients  $R^2$  and standard deviation (s.d.) of the linear relations between CIELAB variables calculated from the results of table 4**

	$\Delta L^*$		$\Delta a^*$		$\Delta b^*$		$\Delta h^*$		$\Delta C^*$		$\Delta E^*$	
	$R^2$	s.d.	$R^2$	s.d.	$R^2$	s.d.			$R^2$	s.d.	$R^2$	s.d.
$\Delta L^*$	-	-	0,03	3,75	0,018	5,92			0,022	6,77		

$\Delta a^*$	0,03	3,75	-	-	0,02	8,2			0,04	6,7	0,002	6,2
$\Delta b^*$	0,018	5,92	0,02	8,2	-	-			0,95	6,77		
$\Delta h^*$							-					
$\Delta C^*$	0,022	6,77	0,04	6,7	0,95	6,77			-	-	0,5	5,03
$\Delta E^*$			0,002	6,2					0,5	5,03	-	-

According to the results in Table 5, the best fit among these relationships is observed in Figure 4E ( $\Delta b^* \rightarrow \Delta C^*$ ), with  $R^2 > 0.95$  and a standard deviation  $s.d. = 6.7$ . This finding is consistent with the results obtained from Panselinos' works; however, in this case, the slope of the linear regression is 0.78. It can be concluded from both cases that the chromatic variable  $\Delta C^*$  exhibits a strong linear correlation with the variable  $\Delta b^*$ . Consequently, the slope of this regression line may represent the unique, individual color signature of each iconographer.

### Application of CIELAB Color Analysis in a Case Study

To evaluate the model's efficacy in identifying an unknown artist, the unsigned frescoes of the Chapel of Saint Eftymios were selected as a case study. The chapel, founded in the 11th century, is situated in the southeast corner of the Basilica of Saint Demetrios in Thessaloniki. Its interior is adorned with numerous unsigned frescoes dating back to 1303 AD. While these works are stylistically classified under the Macedonian School, Professor E.N. Tsigaridas has proposed the hypothesis that their creator was Manuel Panselinos [39, 40]. To empirically validate this attribution, the CIELAB model was applied to fourteen representative frescoes from the chapel (see Figure 5). The analysis aimed to determine whether the chromatic profile of these works aligns with the established "color signature" of Panselinos.



Figure 5: Frescos from the chapel of Saint Eftymiou

The measurement data ( $L^*, a^*, b^*$ ) and the calculated CIELAB variables for the frescoes under study are presented in Table 6. Furthermore, the corresponding linear relationship between  $\Delta b^*$  and  $\Delta C^*$  is illustrated in Figure 6. This figure demonstrates, once again, a highly significant correlation between these two variables, as evidenced by a coefficient of determination  $R^2 = 0.97$ .

Table 6: CIELAB variables for the frescos of Figure

Nº	$\Delta L^*$	$\Delta a^*$	$\Delta b^*$	$\Delta C^*$
1	49,5	4,2	5,2	6,67
2	54,2	2,2	8,0	8,27
3	50,4	2,9	9,2	9,65
4	65,0	1,9	1,6	2,5
5	52,1	3,5	6,4	7,28
6	47,8	1,2	5,4	5,57
7	62,7	1,7	4,3	4,57
8	67,2	1,7	4,7	5,02
9	50,1	1,8	4,5	5,00
10	51,4	1,9	2,6	3,27

11	49,4	-0,6	1,8	1,94
12	51,2	0,7	5,7	5,76
13	52,7	0,9	2,5	2,70
14	47,9	2,9	6,2	6,87

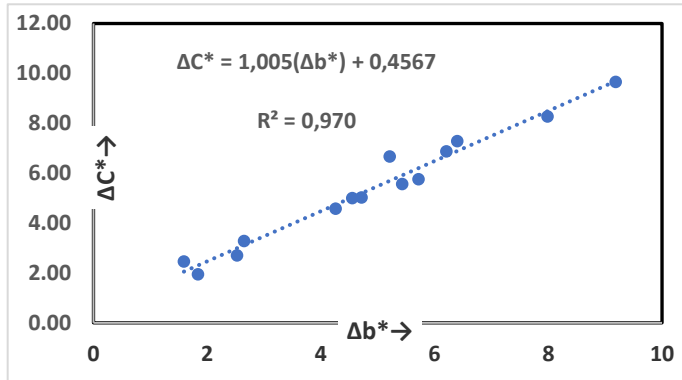


Figure.6: Linear relation between  $\Delta C^*$  and  $\Delta b^*$  from table 6

A comparative analysis of Figures 3E, 4E, and 6 reveals that the regression line for the frescoes in the Chapel of Saint Efthymios aligns significantly more closely with the established profile of Manuel Panselinos than with that of the Astrapas workshop. This high degree of correlation provides compelling empirical evidence supporting the attribution of the Saint Efthymios frescoes to the hand of Manuel Panselinos.

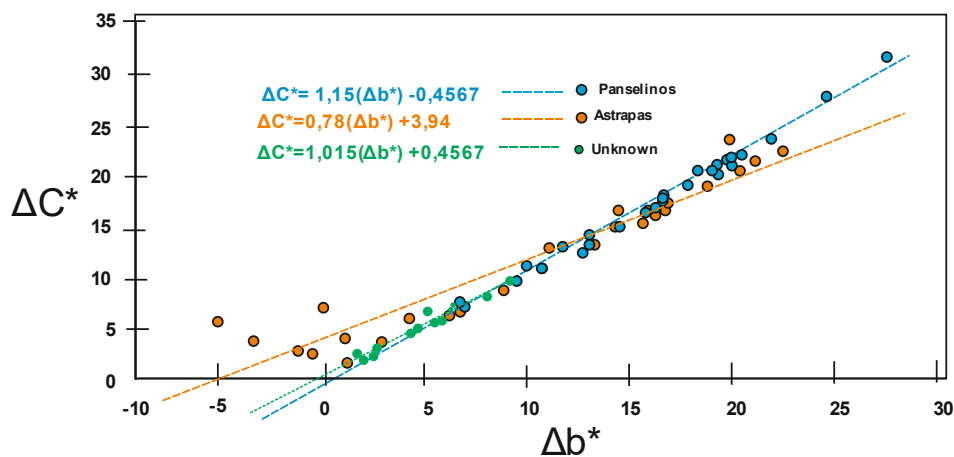


Figure 7: Correlation line of relation  $\Delta C^* \rightarrow \Delta b^*$  for the frescos of chapel of Saint Efthymiou in comparison with the corresponding lines of Panselinos and Astrapa

### Conclusion

The CIELAB analysis of frescoes is proposed as a novel, non-destructive methodology for the preliminary study of art through the chromatic analysis of digital images. This method utilizes rigorous mathematical relationships to reveal the distinct color preferences and stylistic tendencies of an artist. The effective disclosure of these patterns requires the analysis of a statistically significant corpus of work by the same individual. During the comparative analysis of the works of the preeminent 13th-century masters of the Macedonian School—Manuel Panselinos and the duo Michael Astrapas and Eutybios—a strong linear correlation was identified between the variables  $\Delta C^*$  and  $\Delta b^*$ . This relationship proved to be unique for each iconographer, effectively constituting a personal "chromatic identity" (Color ID). The practical utility of this ID was further demonstrated by validating the attribution of the unsigned frescoes in the Chapel of Saint Efthymios in Thessaloniki. Consequently, the development of a comprehensive color database for iconographers would significantly advance the systematic study and authentication of hagiographic art.

## Acknowledgement

The Organic Chemical Technology Lab of National Technical University of Athens for the technological supporting of this research.

## References

- [1] Bozas G. (2021) Codes and Rules in Orthodox hagiography, available from <https://www.pemptousia.gr/video/kodik-es-ke-kanones-stin-agiografia>
- [2] Byzantine Orthodox hagiography, available from <https://www.roussanou.gr/roussanou/spuria/hagiography/>
- [3] Kaminari, A.; Banou, P.; Moutsatsou, A.; and Alexopoulou (2021) A. Non-Destructive Investigation of Paintings on Different Substrates Methodology, Achievements and Limitations. *Design/Arts/Culture* (2),10-21.
- [4] Cartechini, L.; Miliani, C.; Nodari, L.; Rosi, F.; Tomasin, P. (2021) The chemistry of making color in art. *Journal of Cult. Herit* 2021 188-210.
- [5] CIE (1995) Industrial colour-difference evaluation, Technical report 116/1995. In: C.I.d.I.E.C. (ed.) Bureu. CIE, Vienna
- [6] HunterLab (2018) The Basics of Color Perception and Measurement, available from <http://wiki.td-er.n1/images/5/5c/>
- [7] HunterLab (2008) CIE L\* a\* b\* Color Scale. *Application Notes* 8(7):1-4
- [8] McGuire, R.G. (1992) Reporting of objective color measurements. *Hort Science* 27(12):1254-5
- [9] Abbott, J. A. (1999) Quality measurement of fruits and vegetables. *Post-harvest. Biol. Technol.* 15(3), 207-225
- [10] Palechor-Trochez, J.I.; Ordonez Santos, E.L.; and Villada-Castillo, S.H. (2018) Relationship between Color CIEL\*a\*b\* and Total Organic Carbon in Compost. *Adv Mater Sci Eng*, Volume 2018, Article ID5474239: 1-6
- [11] Perkins-Veazie, R.; Collins, J.K.; Pair, S.D.; and Robert, W., (2001) Lycopene content differs among red-fleshed watermelon cultivars. *Journal of the Science of Food and Agriculture* 81: 983-987.
- [12] Tsivas, D.; Vlyssides, A.; and Vlysidis A. (2023) Monitoring of a III-Phase Pomace Composting Process Using the CIELAB Colorimetric Method. *J. Chem Technol Biotechnol* (in press)
- [13] Tsivas, D.; Vlyssides, A.; and Vlysidis A. Monitoring of a III-Phase Pomace Composting Process Using the CIELAB Colorimetric Method. *Waste and Biomass Valorization* 2021,12, 5029-39.
- [14] Ashik Iqbal Khan, M.; Ueno, K.; Horimoto, S.; Komai, F.; Someya, T.; Inoue, K.; Tanaka, K.; and Ono, Y. (2009) CIELAB color variables as indicator of compost stability. *Waste Management* 29: 2969-75.
- [15] Tsivas, D.; Vlyssides, A.; and Vlysidis A. (2023) Differentiation of the composting stages of green waste using the CIELAB color model. *J Chem Technol Biotechnol* 2023: available from <https://onlinelibrary.wiley.com/doi/10.1002/jctb.7370>
- [16] Ricca, M.; Albergina, E.M.; Randazzo L.; Schiavone, S.; Donato, A.; Albanese, P.M.; and La Russa, F. (2021) M. A Combined Non-Destructive Approach to Solving the Forensic Problems in the Field of Cultural Heritage: Two Case Studies. *Appl. Sci.* 11: 6951.
- [17] Leon, K.; Mery, D.; Pedreschi, F.; and Leon, J. (2006) Color measurement in L\*a\*b\* units from RGB digital images. *Food Research International* 39: 1084-1091.
- [18] Luo, M.R.; Cui, G.; Rigg, B., (2001) The development of CIE 2000 color-difference formula, *Color Research and Application* 26: 340-350.
- [19] Sharma, G.; Wu, W; and Dalal, E.N., (2005) The CIED2000 color difference formula: implementation notes, supplementary test data and mathematical observations. *Color Research Application* 30: 21-30.
- [20] Ficher, C; and Kakoulli, I (2006) Multispectral and hyperspectral imaging technologies in conservation: current research and potential applications, *Reviews in Conservation* 7: 3-16
- [21] Brunetti, B; Miliani, C.; Rosi, F.; Doherty, B.; Monico, L.; Romani, A.; and Sgamellotti, A (2016) Non-invasive Investigations of Paintings by Portable Instrumentation: The MOLAB Experience. *Top Cur Chem (Z)* (2016): 374-10.
- [22] Maev, Gr,R.; Gavrilov, D.; Maeva, A.; and Vodyanoy, I. (2008) Modern non-Destructive Physical Methods for Paintings Testing and Evaluation. *Proceedings of 9th International Conference on NDT of Art, Jerusalem Israel, 25-30 May 2008.*
- [23] McGuire, G.R. (1992) Reporting of Objective Color Measurements. *HortScience* 27(12): 1254-1255.
- [24] Orfanides D. (2016) Outdoor sculptures of Thessaloniki, parameters of degradation and deterioration of their materials, MsD Thesis. Aristotle University of Thessaloniki, Thessaloniki.
- [25] Daniel, F.; Mounier, J.; Perez-Arantegui, J.; Pardos, C.; Prieto-Taboada, N.; Fdez-Ortiz de Valehuelo, S; and Castro, K. (2016) Hyperspectral Imaging Applied to Analysis of Gova Paintings in the Museum of Zaragoza. *Journal of Archaeological Science*, 126: 113-120.
- [26] Dyer, J; Verri, G.; and Cupit, J. (2013), *Multispectral Imaging in Reflectance and Photo-induced Luminescence modes: A user manual*, London; The British Museum.
- [27] Kleynhans, T; Messinger, D.W.; Easton, R.L., Jr; Delaney, J.K. (2021) Low-Cost Multispectral System Design for Pigment Analysis in Works of Art. *Sensors*, 21: 5138.
- [28] Liang, H. (2012) Advances in Multispectral and Hyperspectral Imaging system for examining paintings, *Journal of Imaging Science & Technology*, 49: 551.

- [29] Alfeld, M.; and de Viquerie, L. (2017) Recent developments in spectroscopic imaging techniques for historical paintings -A review. *Spectrochimica Acta Part B* 136: 81-105.
- [30] Alin, T. R. (2011). "Master Manu Panselinos and the Macedonian school of painting. *European Journal of Science and Theology*. 7 (1): 13–23
- [31] Daniilia, S.; Tsakalof, A.; Bairachtari, K.; and Chryssoulakis, Y. (2007). "The Byzantine wall paintings from the Protaton Church on Mount Athos, Greece: tradition and science". *Journal of Archaeological Science*. 34 (12): 1971–1984.
- [32] Tsigaridas, Euth. N. (2003). *Manuel Panselinos from the Holy Church of the Protaton*. Athens, Greece: Hagioritiki Estia. p. 5.
- [33] Cutler, A. (1991). "Panselinos, Manuel". In Kazhdan, Alexander (ed.). *The Oxford Dictionary of Byzantium*., Oxford University Press. p. 1572, New York, Oxford
- [34] *Hagiographies of Manuel Panselinos from the-holy church of the protaton 2012* available from: <https://sfantulumteathos.wordpress.com/2012/12/21/manuil-panselinos-frescele-bisericii-protaton-din-karyes-199-fotografii/>
- [35] Pelecanides, S. (1960). The hagiographer Michael Astrapas. *Macedonica* 4(1), 545–547.
- [36] Michael and Eutykhios Astrapas (13ος-14ος century) available from <https://paletaart.wordpress.com/2016/09/26/%CE%B1%CF%83%CF%84%CF%81%CE%B1%CF%80%CE%AC%CF%82-%CE%BC%CE%B9%CF%87%CE%B1%CE%AE%CE%BB-%CE%BA%CE%B1%CE%B9-%CE%B5%CF%85%CF%84%CF%8D%CF%87%CE%B9%CE%BF%CF%82-michael-and-eutykhios-astrapas-13%CE%BF/>
- [37] Cohen, L., Manion, L., Morrison, K. (2007) *Research Methods in Education*, 6th edn. Routledge Farmer, London.
- [38] Snedecor, G.W. and Cochran, W.G. (1989) *Statistical Methods*. 8th Edition, Iowa State University Press, Ames.
- [39] Tsigaridas, N.E. (2016) *Kastoria: Center of painting of Paleologan era (1360-1450)*, Society for Macedonian Studies, Thessaloniki.
- [40] Tsigarida, N.E. (2008) *The frescoes of the chapel of Agios Efthymios (1302/3)*. Pournaras, Thessaloniki
- [41] Vlisidi, A., Doulamis, A., Bakolas and Moropoulou A. (2024) Parametric colour analysis of images from Cretan School of Hagiography (15th – 17th c.AD) using CIELab model. *Scientific Culture*, 10(1): 105-115
- [42] Liu, Juan. (2017) *The Role of Media in Promoting Good Governance and Building Public Perception About Governance: A Comparison of China and the United States*.
- [43] Jenkins, H. (2018). *Convergence culture: Where old and new media collide*. NYU Press.
- [44] Kaur, H., & Randhawa, G. (2021). Media as a tool of public accountability: Implications for education service delivery. *Journal of Public Affairs*, 21(2), e2163. <https://doi.org/10.1002/pa.2163>
- [45] Kim, S., & Lee, J. W. (2017). Enhancing public service performance: The role of human resource management practices. *Public Administration Review*, 77(2), 195–205. <https://doi.org/10.1111/puar.12643>
- [46] Kuhlmann, S., & Wollmann, H. (2014). *Introduction to comparative public administration: Administrative systems and reforms in Europe*. Edward Elgar Publishing.
- [47] Liu, Juan. (2017) *The Role of Media in Promoting Good Governance and Building Public Perception About Governance: A Comparison of China and the United States*.
- [48] Luo, Y., Zhang, L., & Liu, W. (2012). Media coverage and social pressure: Evidence from Chinese government's responses to environmental issues. *Journal of Public Administration Research and Theory*, 23(2), 371–395. <https://doi.org/10.1093/jopart/mus043>
- [49] Moon, M. J. (2002). The evolution of e-government among municipalities: Rhetoric or reality? *Public Administration Review*, 62(4), 424–433. <https://doi.org/10.1111/0033-3352.00196>
- [50] Mu'min, A., & Santosa, A. (2021). Pengaruh kualitas sumber daya manusia dan layanan publik terhadap tata kelola pemerintahan di sektor pendidikan dan kesehatan. *Jurnal Ilmu Administrasi Negara*, 11(2), 112–123.
- [51] Meijer, A. (2021). Government transparency in the age of digital media: Toward a new model. *Government Information Quarterly*, 38(2), 101–110.
- [52] McCombs, M., & Shaw, D. L. (1972). The agenda-setting function of mass media. *Public Opinion Quarterly*, 36(2), 176–187.
- [53] Malhotra, N. K. (2010). *Marketing research: An applied orientation* (6th ed.). Pearson.
- [54] Nasution, A., Lubis, F., & Harahap, R. (2020). Pengaruh pengendalian internal terhadap tata kelola pemerintahan dengan kualitas layanan publik sebagai variabel mediasi. *Jurnal Administrasi Publik*, 17(1), 45–57.
- [55] Na-Nan, K., Chaiprasit, K., & Pukkeeree, P. (2021). Transparency and media in public education services: A pathway to better governance. *Journal of Open Innovation: Technology, Market, and Complexity*, 7(1), 17. <https://doi.org/10.3390/joitmc7010017>

- [56] Neessen, P. C. M., Caniëls, M. C. J., Vos, B., & de Jong, J. P. (2021). The role of the media in educational innovation and public policy change. *Educational Policy*, 35(3), 415–440. <https://doi.org/10.1177/0895904820917780>
- [57] Nguyen, T. V., & Bryant, S. E. (2020). Human resource quality and public service effectiveness in developing countries. *Journal of Public Affairs*, 20(3), e2034. <https://doi.org/10.1002/pa.2034>
- [58] Norris, P. (2000). *A virtuous circle: Political communications in postindustrial societies*. Cambridge University Press.
- [59] Nurhadi. (2019). Peran media massa dalam meningkatkan akuntabilitas birokrasi pelayanan pendidikan di perkotaan. *Jurnal Administrasi Publik*, 16(2), 101–113.
- [60] Nurjanah, N. (2021). Peran media massa dalam membentuk opini publik terhadap kebijakan pendidikan: Kajian deskriptif. Jakarta: Penerbit Ilmu Sosial.
- [61] Norris, P. (2018). *A virtuous circle: Political communications in postindustrial societies*. Cambridge University Press.
- [62] Osborne, S. P., Radnor, Z., & Strokosch, K. (2020). *Public Service Logic: Creating Value for Public Service Users, Citizens, and Society Through Public Service Delivery*. London: Routledge.
- [63] Perry, J. L., & Hondeghem, A. (Eds.). (2008). *Motivation in public management: The call of public service*. Oxford University Press.
- [64] Pandey, S. K., & Wright, B. E. (2006). Connecting the dots in public management: Political environment, organizational goal ambiguity, and the public manager's role ambiguity. *Journal of Public Administration Research and Theory*, 16(4), 511–532. <https://doi.org/10.1093/jopart/mui050>
- [65] Paramitha, D. A. (2024). Pengaruh tata kelola, teknologi informasi, dan kinerja pegawai terhadap penerimaan pajak daerah. *Jurnal Kebijakan dan Administrasi Publik*, 14(1), 65–78.
- [66] Pierre, J., & Peters, B. G. (2000). *Governance, politics and the state*. Macmillan Press.
- [67] Pradipta, R. (2020). Peran media massa dalam pengawasan kebijakan publik sektor pendidikan. *Jurnal Ilmu Komunikasi dan Pemerintahan*, 5(1), 45–58. (Catatan: Tambahkan URL atau DOI jika tersedia)
- [68] Rahman, M. M., & Karim, M. M. (2022). The impact of organizational justice on performance in educational institutions. *Asia Pacific Education Review*, 23(1), 67–81. <https://doi.org/10.1007/s12564-021-09698-6>
- [69] Rhodes, R. A. W. (1996). The new governance: Governing without government. *Political Studies*, 44(4), 652–667. <https://doi.org/10.1111/j.1467-9248.1996.tb01747.x>
- [70] Saragih, F., & Siregar, R. (2021). Pengaruh media lokal terhadap transparansi dan partisipasi publik dalam kebijakan pendidikan di Sulawesi Tenggara. *Jurnal Ilmu Komunikasi*, 19(1), 55–68.
- [71] Sedarmayanti, R., Nurhadi, A., & Fauzan, R. (2020). Good governance dan kinerja birokrasi publik: Perspektif layanan publik. *International Journal of Academic Research in Business and Social Sciences*, 10(5), 123–135. <https://doi.org/10.6007/IJARBS/v10-i5/12345>
- [72] Sulistiyani, A. T., & Hidayat, R. (2018). Pengaruh kualitas sumber daya manusia terhadap kinerja pelayanan publik di sektor pendidikan. *Jurnal Administrasi Publik*, 15(1), 25–36. <https://doi.org/10.20473/jap.v15i1.2018.25-36>
- [73] Tandoc Jr., E. C., & Johnson, E. (2016). Most students get breaking news first from Twitter. *New Media & Society*, 18(9), 1236–1253. <https://doi.org/10.1177/1461444814553795>
- [74] Tuan, L. T., Thao, N. T. T., & Nhi, N. T. Y. (2021). Public service quality and citizen satisfaction: Evidence from the education sector. *Public Services Quarterly*, 17(4), 321–339. <https://doi.org/10.1080/15228959.2021.1871979>
- [75] UNESCO. (2021). *Global Education Monitoring Report 2021: Non-State Actors in Education: Who Chooses? Who Loses?* UNESCO Publishing.
- [76] UNDP. (2018). *Governance for Sustainable Development: Integrating Governance in the Post-2015 Development Framework*. United Nations Development Programme.
- [77] Vannala, P. (2022). Good governance as a mediating factor in the relationship between media, human resources, and public service performance. *International Journal of Public Sector Management*, 35(5), 513–529. <https://doi.org/10.1108/IJPSM-11-2021-0302>
- [78] Wikansari, R., Sayuti, M., Sipayung, B., Defitri, S. Y., Luturmas, Y., & Kenney, L. M. (2023). Implementation of Integrated One Stop Model in Public Services: An Analysis of Human Resources Performance Competency Development in The Indonesian Government Sector. *Multicultural Education*, 9(1), 16–27
- [79] Wright, B. E., Moynihan, D. P., & Pandey, S. K. (2007). Pulling the levers: Transformational leadership, public service motivation, and mission valence. *Public Administration Review*, 67(1), 54–64. <https://doi.org/10.1111/j.1540-6210.2006.00695.x>
- [80] WHO. (2020). *Delivering quality health services: A global imperative for universal health coverage*. World Health Organization. <https://apps.who.int/iris/handle/10665/272465>
- [81] World Bank. (2019). *World development report 2019: The changing nature of work*. World Bank Group. <https://www.worldbank.org/en/publication/wdr2019>
- [82] World Bank. (2019). *World Development Report 2018: Learning to Realize Education's Promise*. World Bank Group.

- [83] Yudiatmaja, D. (2021). Persepsi publik dan peran media dalam pembentukan kebijakan layanan. *Policymaking: Government and Research*, 3(2), 45–60.
- [84] Zandi, G., Nadarajah, D., & Gharleghi, B. (2019). Human resource management practices and organizational performance: The mediating role of knowledge sharing and motivation in the public sector. *International Journal of Public Administration*, 42(7), 590–600. <https://doi.org/10.1080/01900692.2018.1498103>.